DEVELOPMENT OF THE MODEL OF A SELF EXCITED LOOP

Gopal Joshi, BARC, Mumbai, India
Vivek Agarwal, Girish Kumar, IITB, Mumbai, India
R.G. Pillay, DNAP, TIFR, Mumbai, India

Abstract

As a first step towards development in digital domain, a computer model of a self excited loop (SEL) has been created using MATLAB/SIMULINK. The behaviour of a resonator and a power amplifier combination has been approximated using two first-order differential equations. The square of the amplitude of the RF field in the resonator acts as a driving force for the motion of mechanical modes of the resonator, which are individually represented as second order systems. A key element is the limiter, which has been modelled as a feedback loop, to achieve constant output amplitude. The model has been created in the I-Q domain for computational efficiency and close correspondence with actual implementation. To study the field stabilisation, proportional amplitude and phase feedback loops have been appended to the model of the SEL. In this paper we discuss the details of the model and results from simulation. Initial experimental results are also presented.

INTRODUCTION

A self excited loop (SEL) serves as a very convenient basis for setting up and subsequent amplitude and phase locking of the RF fields in a super-conducting resonator [1]. Fig. 1 shows the essential elements of an SEL. The output of the resonator is fed back to its input via a limiter and a phase shifter in cascade. The attenuator and the power amplifier are used to set up a specific field in the resonator. For amplitude and phase locking, a controller is appended to the basic SEL.
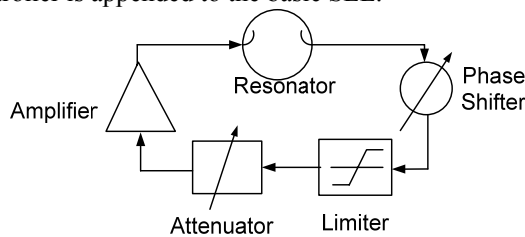
Figure 1: Elements of a Self Excited Loop.

RF control systems based on the implementation of an SEL in the analog domain have been in use for many years [2, 3]. A successful implementation of SEL in digital domain has only been recently reported [4]. To upgrade the low-level RF control of the Pelletron-Linac Facility at TIFR, an SEL based system is being developed in the digital domain. As a first step towards this development, a computer model of an SEL has been created using MATLAB/SIMULINK. For the model development and subsequent experimentation, we have selected the architecture of the low level signal processing blocks, viz.: the limiter, controller, phase shifter, etc, and

implemented these in the I-Q domain. In the following sections we explain the model and present results from the simulations along with those from initial experiments.

MODEL

For superconducting cavities which have a very high quality factor, an approximate differential equation describing the resonator field, represented as a complex phasor V, can be derived [5] as:

$$\tau_0 \frac{dV}{dt} + (1 + j(\omega - \omega_0)\tau_0)V = V_{ext} \tag{1}$$

where, ω_0 is the resonant frequency of the cavity and τ_0 is the intrinsic decay time constant. V_{ext} represents the net phasor due to external excitations, viz.: the high power RF amplifier coupled to the resonator via a transmission line and the beam current. An equivalent circuit for this part is shown in Fig. 2.
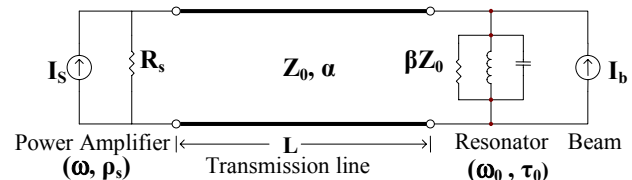
Figure 2: Equivalent Circuit of the RF power system.

Decomposing the various phasors into the in-phase and quadrature components the following set of first order differential equations model the dynamics of the voltage in the resonator:

$$\frac{dI}{dt} = -\frac{1}{\tau}I - \Delta\omega Q + \frac{1}{\tau}\frac{\beta}{\beta+1}(2V_{fi} + Z_0 I_{bi}) \tag{2}$$

$$\frac{dQ}{dt} = -\frac{1}{\tau}Q + \Delta\omega I + \frac{1}{\tau}\frac{\beta}{\beta+1}(2V_{fq} + Z_0 I_{bq}) \tag{3}$$

where, (I, Q), (V_{fi}, V_{fq}) and (I_{bi}, I_{bq}) are the in-phase and quadrature components of the voltage on the resonator, forward wave and beam current, respectively. τ is the loaded decay time constant, $\Delta\omega = (\omega_0 - \omega)$ is the detuning parameter and β is the coupling constant.

The RF source is modelled as a generator of a forward wave V_f as:

$$V_f = \frac{(1-\rho_s)}{2}R_s I_s + \rho_s V_r \tag{4}$$

where, ρ_s is the source reflection coefficient. The phasor V_o representing the output of the transmission line is related to that at the input V_i by the following transformation:

$$V_0(t) = e^{-(\alpha + \frac{j\omega}{c})L}V_i(t - \frac{L}{c}) \tag{5}$$

where, L is length of the line, α is the attenuation constant and c is the electromagnetic wave velocity. The model of the complete high-power RF system is derived by suitably connecting the models of RF power source, transmission line and the resonator as described in [6].
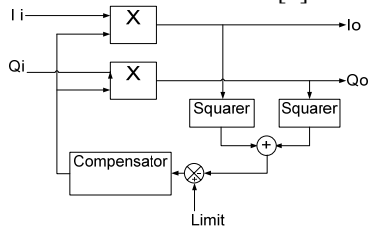
Figure 3: Architecture of the Limiter.

The limiter is a crucial element of the low-level RF system and it has been implemented as a feedback loop, which keeps the output amplitude constant by multiplying a suitable real number to both the I and the Q components of the input. Fig. 3 shows the architecture of the limiter which has been modelled as a discrete time process and computations carried out with finite precision. The only essential dynamical element present in the feedback loop is a delay, which equals the number of clock time periods required to complete the computations. In order to improve both the static and the dynamic behaviour due to this pure delay process, a suitable compensation is needed in the loop. We have used a single pole IIR filter for this purpose.

With the limiter implemented as described above, we have two interacting closed loops in a free running SEL. The behaviour of the loop in the limiter is like that of a high pass filter, while the outer SEL loop behaves like a low pass filter. For a good transient response of this composite system around the equilibrium point, the gain due to the outer loop should start decreasing at frequencies sufficiently below that at which the gain of the loop in the limiter starts to increase.

The availability of modern programmable digital hardware having both high precision and high speed, the condition mentioned above can be easily met even for moderately high-Q cavities.
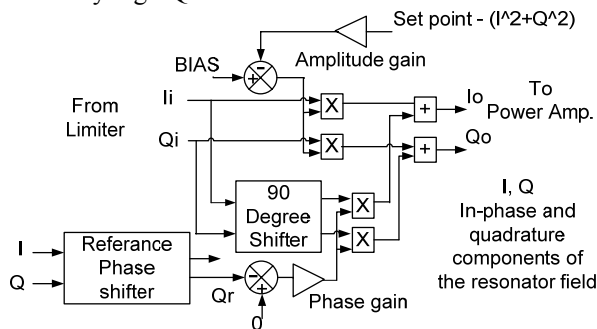
Figure 4: The Controller.

The controller architecture is shown in fig. 4. The phase and the amplitude locks are achieved by appropriate modulation of the drive to the resonator. The I-Q components of the resonator field are phase shifted by the reference phase angle. Thus, comparing the resultant quadrature component to zero represents the phase error. The amplitude error is generated by comparing the square of the field amplitude with a suitable set-point. A bias can also be introduced to set the quiescent operating point.

The phase shifters in the I-Q domain are represented by a rotation transformation, corresponding to a phase angle ϕ. Thus, the output V_o is related to that at the input V_i as:

$$V_o = V_i e^{j\phi} \qquad (6)$$

It can be shown that the dynamics of the shift in resonant frequency of the resonator, due to the various mechanical modes excited by the radiation pressure in the cavity, can be represented by a second order differential equation [1, 5, 7] as:

$$\frac{d^2\omega_\mu}{dt^2} + \frac{2}{\tau_\mu}\frac{d\omega_\mu}{dt} + \Omega_\mu^2\omega_\mu = -K_\mu\Omega_\mu^2 VV^* \qquad (7)$$

where, Ω_μ and τ_μ are the fundamental frequency and decay time constant, respectively, of a particular mechanical mode. The square of the resonator field amplitude $(VV^* = I^2 + Q^2)$ drives the mechanical mode and ω_μ is the corresponding shift in resonant frequency.

In general, the total change in the resonant frequency due to electromechanical coupling is obtained by summing the individual contributions of all excited modes. The electrical and mechanical systems are connected to each other by the following relation:

$$\omega_0 = \omega_{00} + \sum \omega_\mu + \omega_{ext} \qquad (8)$$

where, ω_{00} is the centre frequency of the resonator at zero field and ω_{ext} is the resonant frequency change due to external mechanical perturbations.

Model of the Complete SEL and Test Results

The model of the SEL is completed by concatenating the models of individual sub-systems and by incorporating suitable gain, attenuation, delay of the processing and interconnects, as well as the saturation effect in the power amplifier. MATLAB/SIMULINK has proved a very convenient tool for modelling the SEL, a part of which is analog and the other part a finite precision, discrete time system.

Various operating scenarios can be easily created using this model. Fig. 5 shows the result obtained for one such example. The system is turned on at time $t = 0$ by injection of a pulse in the in-phase component to the resonator. The initial detuning of one loaded band-width reduces with time due to electromechanically induced resonant frequency change. Phase feedback is introduced at 6 ms and the system attains phase lock at -90° phase angle. During the initial period following the closure of phase feedback, the drive is not sufficient to keep the amplitude constant. This leads to a dip in the resonator field value, which in turn excites the mechanical mode in the resonator. Amplitude feedback is turned on at 8 ms and as the drive power is sufficient to handle the frequency excursions, both the locks are retained. It should be noted that the output amplitude of the limiter

remains relatively unaffected by the transients mentioned above.
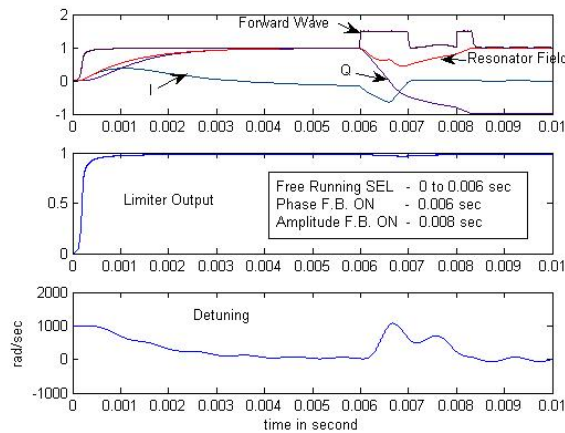
Figure 5: A sample run.

The parameters used for the above simulation are: resonator: $\tau = 0.001$s, initial $\Delta\omega = 1000$rad/s, $\beta = 1$, $\tau_\mu = 0.01$s, $\Omega_\mu = 2\pi(1000)$rad/s, $K_\mu = 1000$ per (volts)^2, compensator (filter) in the limiter loop $f(z) = 0.04/(1-0.999/z)$; the computational delay in the feedback loop of limiter is 4 samples with a sampling time of 25ns, amplitude feedback gain = 20, phase feedback gain = 20, loop phase shift = 0, reference phase shift = 90°, and amplitude reference = 1.

Initial Experiments
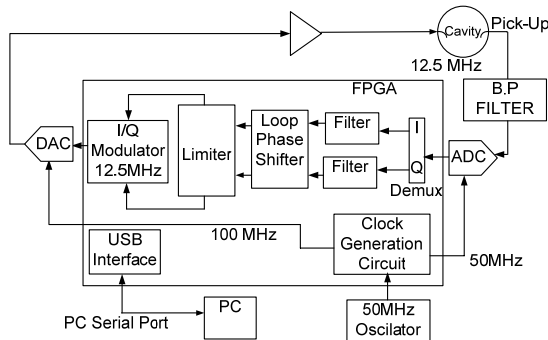
Figure 6: Experimental Set-up.

We have realised a free running SEL using Altera Cyclone III FPGA development kit. Fig. 6 shows the scheme which is being tested at low power levels with a normal-conducting resonator having a decay time of about 12µs. Fig. 7 shows an oscilloscope trace of the resonator pick-up after the application of a trigger signal, which resets the system. The oscillations in the loop are initiated by the intrinsic noise of the set-up.

In near future, we plan to build a complete system by appending up/down converters and a proper clocking system. For the final system, the resonator pickup will be down-converted to 20MHz. This choice is based on a compromise between low-latency and accurate field detection. The complete signal processing has been successfully simulated and synthesised for an FPGA with

ADC samples at 80MHz (four samples per cycle), leading to I-Q data streams at 40MHz and thus a processing period of 25ns.
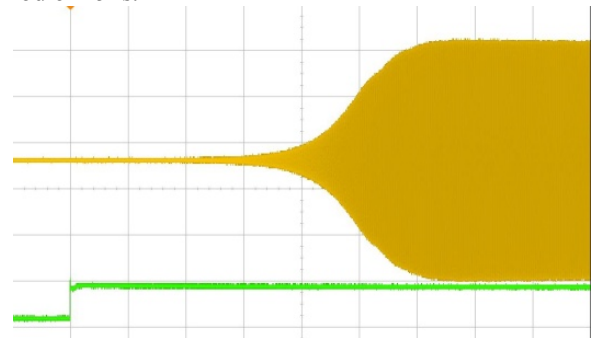
Figure 7: Self Excited Oscillations, 10µs per div.

CONCLUSION

The behaviour of the model for resonator control has been successfully demonstrated. The results from initial experiments using a development kit (processing period of 40ns) are encouraging. The SEL based RF control in digital domain will be tested on the super-conducting resonators at TIFR.

ACKNOWLEDGEMENTS

REFERENCES

[1] J.R. Delayen, "Phase and Amplitude Stabilisation of Super-conducting Resonators", Ph.D. Thesis, Caltech (1978).
[2] Ben-Zvi et al, "The Control and Electronics of a Superconducting Booster Module", Nuclear Instruments and Methods in Physics, A245, p. 1-12 (1986).
[3] G. Joshi et al, "Resonator Controller for the Superconducting LINAC", Proceedings of Symposium on Intelligent Nuclear Instrumentation 2001, p. 105-110 (2001).
[4] Allison et al, "A Digital Self Excited Loop for Accelerating Cavity Field Control", PAC07 (2007).
[5] D. Shulze, "Ponderomotive Stability of RF Resonators and Resonator Control systems", ANL-Trans-944 (1972).
[6] B.R. Cheo et al, "Dynamic Interactions between RF Sources and LINAC cavities with Beam Loading", IEEE Transactions – Electron Devices, Vol. 38, No. 10, p. 2264-2274 (1991).
[7] J.R. Delayen, "Ponderomotive Instabilities and Microphonics – a Tutorial", Phisica C 441, p. 1-6, (2006)